Proceedings of the Estonian Academy of Sciences,
2015, **64**, 3, 270–277
doi: 10.3176/proc.2015.3.10
Available online at www.eap.ee/proceedings

Nonlinear evaluation of the kinematics of directional field waves

John Grue

University of Oslo, Department of Mathematics, PO Box 1053 Blindern, NO-0316 Oslo, Norway; johng@math.uio.no

Received 8 December 2014, accepted 7 May 2015, available online 20 August 2015

Abstract. A nonlinear calculation procedure for obtaining the wave kinematics from elevation measurements from field data is outlined in detail. A horizontal current is accounted for. The numerical calculations from the field data are compared to the kinematics of random waves obtained in laboratory measurements.

Key words: nonlinear calculations, orbital velocity, directional field waves, wave kinematics, PIV from laboratory.

1. INTRODUCTION

The mathematical analysis and wave kinematics calculations presented in this paper are motivated by a set of ocean wave measurements where the elevation was obtained and there was a need to calculate the kinematics that was not measured. A particular motivation for obtaining the kinematics was to interpret the wave breaking, which was measured as part of the field measurement. The Gulf of Tehuantepec experiment (GOTEX) obtained, by airborne lidar measurements, the wave elevation over swaths 5 km long and 200 m wide. The resolution was 5 m in each direction (see [6]). The waves were driven by a strong offshore wind. The elevation, η, was obtained over horizontal regions as a function of the coordinate in the two horizontal directions. The waves co-propagated with a strong horizontal current. A sample of the elevation measurement is shown in Fig. 1a. The kinematics of the wave elevation sample is evaluated here. The gradient of the sea, $\nabla\eta$, illustrates the level of the nonlinearity (Fig. 2). It is seen that the local elevation gradient is down to -0.32 at $x_1 = 4730$ m. In [4] two different swaths of the directional field waves from GOTEX were analysed. The computations were compared to unidirectional irregular laboratory waves obtained in conditions with no wind, examining the breaking threshold in the laboratory conditions.

The main point has been to calculate the fluid velocity from a set of elevation measurements. In the present paper we outline the details of the mathematical derivation for obtaining the wave kinematics from elevation measurements. We obtain the kinematics of several local wave events in one of the swaths from GOTEX. The calculated kinematics is compared to irregular wave events obtained in laboratory. Similarities are pointed out.

2. CALCULATIONS BASED ON INTEGRAL EQUATIONS

The purpose of the mathematical–numerical method is to evaluate the wave-induced kinematics from data sets of elevation measurements obtained in the field. The time-derivative of the surface elevation obtained in space is required. The effect of a horizontal current is accounted for in the analysis. Horizontal coordinates

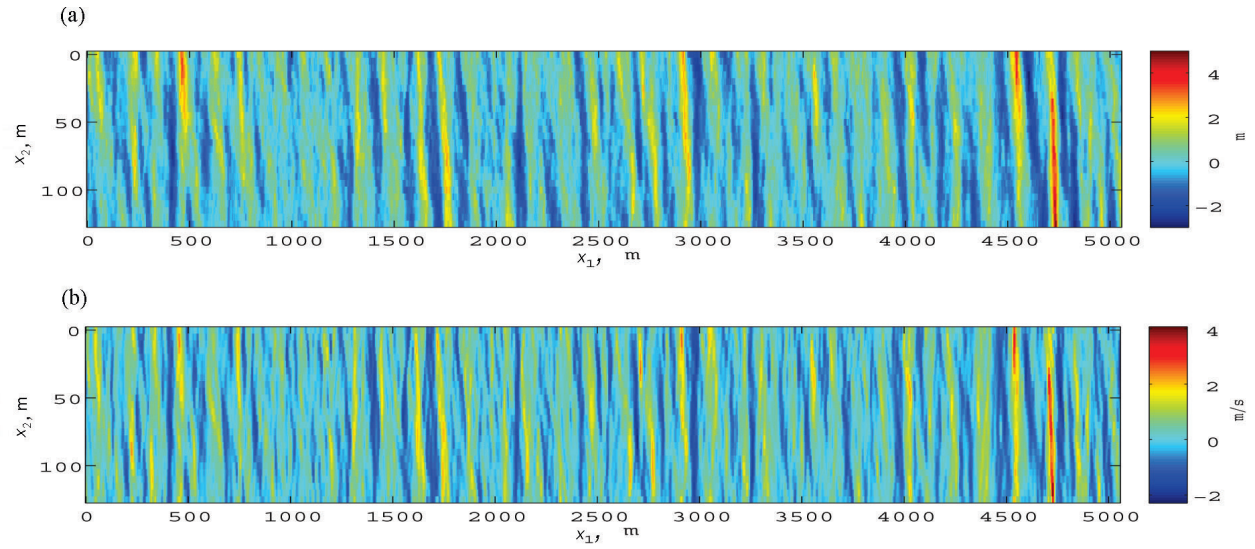

Fig. 1. (a) Elevation in a sample of directional field waves from the GOTEX experiment [6] and (b) calculated velocities u_1 of this sample.

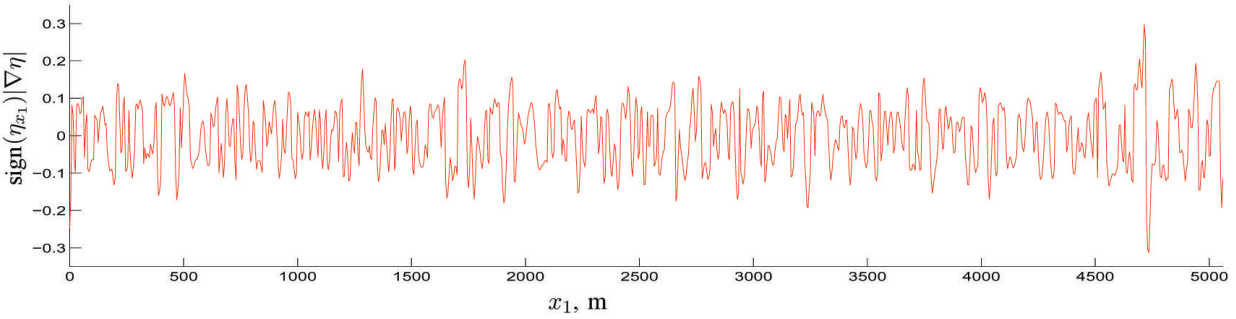

Fig. 2. Plot of sign$(\eta_{x_1})|\nabla\eta|$ of the elevation in Fig. 1a along $x_2 = 120$ m.

$\mathbf{x} = (x_1, x_2)$ are introduced with the x_1-direction along the main wave direction and x_2 laterally. The vertical coordinate is denoted by y. The fluid velocity $\mathbf{v}'$ is assumed to be composed by the wave-induced velocity, obtained by $\nabla\phi$, where ϕ is a velocity potential, plus a horizontal current $\mathbf{U} = (U_1, U_2)$. This means that

$$\mathbf{v}' = \nabla\phi + \mathbf{U} = (u_1 + U_1, u_2 + U_2, \phi_y) = (u_1', u_2', \phi_y), \tag{1}$$

where $u_1' = u_1 + U_1$ and $u_2' = u_2 + U_2$.

The kinematic boundary condition at the position of the wave surface $y = \eta$ reads

$$\frac{\partial\phi}{\partial y} = \frac{\partial\eta}{\partial t} + (\mathbf{U} + \nabla\phi)\cdot\nabla\eta, \tag{2}$$

where t denotes time. Alternatively, this condition may be formulated in terms of the normal velocity of the wave surface, $\partial\phi/\partial n$, by

$$\frac{\partial\phi}{\partial n}(1 + |\nabla\eta|^2)^{1/2} = \frac{\partial\phi}{\partial y} - \nabla\phi\cdot\nabla\eta = \frac{\partial\eta}{\partial t} + \mathbf{U}\cdot\nabla\eta = \frac{\partial\zeta}{\partial t}, \tag{3}$$

where the latter defines $\zeta_t = \eta_t + \mathbf{U}\cdot\nabla\eta$, and where n denotes the upward normal along the surface.

Let $\Phi(\mathbf{x},t) = \phi(\mathbf{x}, y = \eta(\mathbf{x},t), t)$ denote the velocity potential evaluated at the wave surface. The horizontal velocity at the surface is obtained by $\nabla_{\mathrm{H}}\phi|_{y=\eta}$, where ∇_{H} denotes horizontal gradient. Using that

$$\nabla_{\mathrm{H}}\Phi(\mathbf{x}) = \nabla_{\mathrm{H}}\phi(\mathbf{x}, y = \eta(\mathbf{x})) = (\nabla_{\mathrm{H}}\phi)|_{y=\eta} + \frac{\partial\phi}{\partial y}\nabla_{\mathrm{H}}\eta,$$

we obtain $(u_1, u_2) = \nabla_{\mathrm{H}}\Phi - (\partial\phi/\partial y)\nabla_{\mathrm{H}}\eta$, where

$$\frac{\partial\phi}{\partial y} = \zeta_t + \nabla_{\mathrm{H}}\Phi\cdot\nabla_{\mathrm{H}}\eta - \frac{\partial\phi}{\partial y}|\nabla_{\mathrm{H}}\eta|^2,$$

giving

$$(u_1, u_2) = \nabla_{\mathrm{H}}\Phi - \frac{\eta_t + (\mathbf{U} + \nabla_{\mathrm{H}}\Phi)\cdot\nabla_{\mathrm{H}}\eta}{1 + |\nabla_{\mathrm{H}}\eta|^2}\nabla_{\mathrm{H}}\eta, \tag{4}$$

which obtains (u_1, u_2), accounting for a horizontal current $\mathbf{U}$.

Let the water depth be infinite. The potential Φ along the surface is obtained from the Laplacian velocity potential ϕ. The latter is obtained using Green's theorem to ϕ and a Green function where the latter is the three-dimensional source function given by $1/r$; r is the difference between the evaluation point $(\mathbf{x}, y)$ and the source point $(\mathbf{x}', y')$, i.e. $r = |(\mathbf{x}', y') - (\mathbf{x}, y)|$. With the field point on the wave surface, we obtain

$$2\pi\phi(\mathbf{x}, y) = \int_{F+S_{\mathrm{c}}} \Big(\frac{\partial\phi'}{\partial n'}\frac{1}{r} - \phi'\frac{\partial}{\partial n'}\frac{1}{r}\Big)dS', \tag{5}$$

where F denotes the wave surface and S_{c} a control surface such that F and S_{c} enclose the fluid volume in consideration. The normal vector n is pointing out of the fluid, a prime denotes integration variable, and $\phi' = \phi(\mathbf{x}', y')$, etc. It is assumed that there is no fluid motion at the control surface, thus the only contribution to the integral on the right-hand side of (5) is from the wave surface F.

Following [1] (section 6), [3] (section 6), and [2], the Green function is obtained by

$$\frac{1}{r} = \frac{1}{R}\Big(1 + \frac{(y'-y)^2}{R^2}\Big)^{-1/2} = \frac{1}{R} - \frac{1}{2}\frac{(y'-y)^2}{R^3} + \Big[\frac{1}{r} - \frac{1}{R} + \frac{1}{2}\frac{(y'-y)^2}{R^3}\Big], \tag{6}$$

where $R = |\mathbf{R}|$ and $\mathbf{R} = \mathbf{x}' - \mathbf{x}$ denotes horizontal distance. In (6), for $y' = \eta'$ and $y = \eta$, $(\eta' - \eta)^2/R^2 \to (\partial\eta/\partial R)^2$ for $R \to 0$ and $(\eta' - \eta)^2/R^2 \to 0$ for $R \to \infty$. In the present application the local wave slope is up to about 0.3, and $(\partial\eta/\partial R)^2$ up to about 0.1. The leading contribution from the square brackets on the right-hand side of (6) is $O((\partial\eta/\partial R)^4/R)$.

The contribution from the dipole in (5) becomes

$$\frac{\partial}{\partial n'}\frac{1}{r} = -\Big(1 + \frac{(\eta'-\eta)^2}{R^2}\Big)^{-3/2}\nabla'\cdot\Big((\eta'-\eta)\nabla'\frac{1}{R}\Big)\sqrt{1 + |\nabla'\eta'|^2}. \tag{7}$$

The integral equation (5) becomes

$$2\pi\Phi = \int_{\mathbf{x}'}\Big[\Big(\frac{1}{R} - \frac{1}{2}\frac{(\eta'-\eta)^2}{R^3}\Big)\frac{\partial\zeta'}{\partial t} + \Phi'\Big(1 + \frac{(\eta'-\eta)^2}{R^2}\Big)^{-3/2}\nabla'\cdot\Big((\eta'-\eta)\nabla'\frac{1}{R}\Big)\Big]d\mathbf{x}', \tag{8}$$

where integration is over the horizontal plane, and where (3), (6), and (7) and $dS' = \sqrt{1 + |\nabla'\eta'|^2}d\mathbf{x}'$ have been used. In the first inner parentheses on the right-hand side of (8) terms of the fifth order in the wave slope are left out.

The leading contribution to the integral equation becomes

$$2\pi\Phi = \int_{\mathbf{x}'} \frac{1}{R}\frac{\partial \zeta'}{\partial t} d\mathbf{x}'. \tag{9}$$

This obtains the potential as an integral over the wave surface, of the time derivative of the wave elevation. We now use the transform

$$\frac{1}{R} = \mathscr{F}^{-1}\Big(\frac{2\pi}{k} e^{-\mathrm{i}\mathbf{k}\cdot\mathbf{x}'}\Big), \tag{10}$$

where $\mathscr{F}$ denotes Fourier transform, $\mathscr{F}^{-1}$ inverse Fourier transform, $\mathbf{k} = (k_1, k_2)$ horizontal wavenumber in spectral space, and $k = |\mathbf{k}|$. Replacing in (9) $1/R$ by its inverse Fourier transform and interchanging the order of integration, we obtain

$$\int_{\mathbf{x}'} \frac{1}{R}\frac{\partial \zeta'}{\partial t} d\mathbf{x}' = \mathscr{F}^{-1}\Big(\frac{2\pi}{k}\int_{\mathbf{x}'} \frac{\partial \zeta'}{\partial t} e^{-\mathrm{i}\mathbf{k}\cdot\mathbf{x}'} d\mathbf{x}'\Big) = 2\pi\mathscr{F}^{-1}(\mathscr{F}(\zeta_t)/k). \tag{11}$$

Obtaining the Fourier transform of (9) gives

$$\mathscr{F}(\Phi) = \mathscr{F}(\zeta_t)/k. \tag{12}$$

The quadratic contribution to the right-hand side of (8) reads

$$-\int_{\mathbf{x}'} (\eta' - \eta)\nabla'\Big(\frac{1}{R}\Big)\cdot\nabla'\Phi' d\mathbf{x}', \tag{13}$$

where Gauss's theorem over the horizontal plane is used, assuming no contributions from a far field line integral, and $(1+(\eta'-\eta)^2/R^2)^{-3/2}$ has been put to unity. Inserting $\nabla'(1/R) = \mathscr{F}^{-1}(2\pi(-\mathrm{i}\mathbf{k}/k)e^{-\mathrm{i}\mathbf{k}\cdot\mathbf{x}'})$ and interchanging the order of integration, (13) becomes

$$\begin{aligned} 2\pi\mathscr{F}^{-1}\Big(\frac{\mathrm{i}\mathbf{k}}{k}\cdot\int_{\mathbf{x}'}\eta'\nabla'\Phi' e^{-\mathrm{i}\mathbf{k}\cdot\mathbf{x}'} d\mathbf{x}'\Big) + 2\pi\eta\mathscr{F}^{-1}\Big(\frac{(\mathrm{i}\mathbf{k})\cdot(-\mathrm{i}\mathbf{k})}{k}\int_{\mathbf{x}'}\Phi' e^{-\mathrm{i}\mathbf{k}\cdot\mathbf{x}'} d\mathbf{x}'\Big) \\ = 2\pi\mathscr{F}^{-1}\Big(\frac{\mathrm{i}\mathbf{k}}{k}\cdot\mathscr{F}(\eta\nabla\Phi)\Big) + 2\pi\eta\mathscr{F}^{-1}[k\mathscr{F}(\Phi)]. \end{aligned} \tag{14}$$

In the cubic contribution on the right-hand side of (8) we insert $1/R^3 = \nabla'^2(1/R) = 2\pi\mathscr{F}^{-1}(-ke^{-\mathrm{i}\mathbf{k}\cdot\mathbf{x}'})$, giving

$$\begin{aligned} -\pi\int_{\mathbf{x}'}\mathscr{F}^{-1}(-ke^{-\mathrm{i}\mathbf{k}\cdot\mathbf{x}'})(\eta^2 - 2\eta\eta' + \eta'^2)\zeta_t' d\mathbf{x}' \\ = \pi\eta^2\mathscr{F}^{-1}(k\mathscr{F}(\zeta_t)) - 2\pi\eta\mathscr{F}^{-1}(k\mathscr{F}(\eta\zeta_t)) + \pi\mathscr{F}^{-1}(k\mathscr{F}(\eta^2\zeta_t)). \end{aligned} \tag{15}$$

Together, the contributions from (12), (14), and (15) provide the cubic approximation of the fully nonlinear integral equation (5), obtaining $\nabla\Phi$ from $\mathscr{F}^{-1}[\mathrm{i}\mathbf{k}\mathscr{F}(\Phi)]$, where

$$\begin{aligned} k\mathscr{F}(\Phi) &= \mathscr{F}(\zeta_t) + k\mathscr{F}\Big(\eta\mathscr{F}^{-1}[k\mathscr{F}(\Phi)]\Big) + \mathrm{i}\mathbf{k}\cdot\mathscr{F}(\eta\nabla\Phi) \\ &\quad + \frac{k}{2}\mathscr{F}\{\eta^2\mathscr{F}^{-1}[k\mathscr{F}(\zeta_t)]\} - k\mathscr{F}\{\eta\mathscr{F}^{-1}[k\mathscr{F}(\zeta_t\eta)]\} + \frac{1}{2}k^2\mathscr{F}(\zeta_t\eta^2) + h.n.t., \end{aligned} \tag{16}$$

whereby (4) is evaluated. In (16) *h.n.t.* means quartic and higher order nonlinear terms. The contributions from a current in (16) appear in the linear and cubic terms through $\zeta_t = \eta_t + \mathbf{U}\cdot\nabla_H\eta$.

3. RESULTS

In the GOTEX experiment, wave elevation was obtained by a combined measurement in the front and aft of the recording airplane. This enables evaluation of the time derivative of the surface elevation, i.e., $\partial\eta/\partial t$ as a function of the horizontal coordinates (x_1, x_2) of the swaths. The functions are used as input to Eq. (16). The fluid velocity is then evaluated using Eq. (4). The calculated velocity u_1 from the elevation measurement in Fig. 1a is shown in Fig. 1b. The range of u_1 is between -2.5 m/s and 4 m/s.

A characteristic wavenumber is evaluated in order to establish a velocity scale. The rms-value of the elevation and elevation gradient shown in Fig. 1a are obtained by $(\overline{\eta^2})^{1/2} = 0.89$ m and $(\overline{|\nabla\eta|^2})^{1/2} = 0.080$, respectively, where the bar denotes average over all elevation points. An average wavenumber of the sea may be estimated by $k_{\text{av}} = \left(\overline{|\nabla\eta|^2}\right)^{1/2} / \left(\overline{\eta^2}\right)^{1/2} = 0.089$ m^{-1}. A reference wave phase speed may be obtained by

$$c_{\text{av}} = \sqrt{g/k_{\text{av}}} + U_1,$$

where the effect of a current is accounted for. This is measured in the field measurement, along the x_1-direction of the swath [6]. Figure 3 plots the horizontal fluid velocity normalized by $c_{\text{av}} = \sqrt{g/k_{\text{av}}} + U_1 = 11.5$ m/s, where a measured current of $U_1 = 1$ m/s is included. The nondimensional velocity is up to 0.44 for $x_1 = 4730$ m, which is a very strong nondimensional horizontal fluid velocity. Linear and nonlinear calculations show noticeable differences in the local wave phase and at the large events.

We also define a local wave celerity of a local wave event of the wave field by

$$c_{\text{local}} = \sqrt{(g/k_{\text{local}})(1+\varepsilon_{\text{local}}^2)} + U_1.$$

In this expression the local wave slope, $\varepsilon_{\text{local}}$, is taken as the local maximum of $|\nabla\eta|$. As an example, in one of the events that are analysed, $|\nabla\eta|_{\max}$ is 0.32 for the local wave. A local wavenumber of the event is calculated using

$$k_{\text{local}}\eta_{\max} = \varepsilon_{\text{local}} + \frac{1}{2}\varepsilon_{\text{local}}^2 + \frac{1}{2}\varepsilon_{\text{local}}^3, \tag{17}$$

where $\eta_{\max}$ is the maximum local elevation, see [5]. In the field-waves (Fig. 1a), the large event at $x_1 = 4730$ m and $x_2 = 120$ m has a maximum elevation of $\eta_{\max} = 4.7$ m. For this event we obtain $k_{\text{local}} = 0.081$ m^{-1} and $c_{\text{local}} = 12.6$ m/s (with $U_1 = 1$ m/s), which is 10% higher than the linear estimate based on the global wavenumber of the wave series. The calculation gives $(u_1, u_2) = (4.02, 0)$ m/s at maximum (at $x_1 = 4730$ m and $x_2 = 120$ m). In nondimensional terms we obtain $|(u_1 + U_1, u_2)|_{\max}/c_{\text{local}} = 0.40$, which is 10% lower than the estimate based on c_{av}. See also the hodograph plot in Fig. 4. Note, while

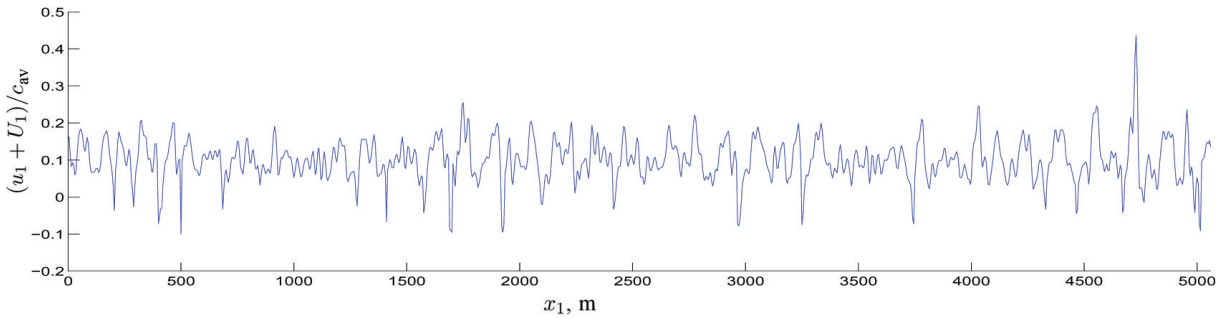

Fig. 3. Plot of $(u_1 + U_1)/c_{\text{av}}$ calculated from the elevation in Fig. 1a along x_2 = 120 m.

$k_{\text{local}} = 0.081$ m^{-1} for this local wave event is rather close to the global average of $k_{\text{av}} = 0.089$ m^{-1}, there is generally a large difference between the local wavenumbers k_{local} of the different wave events, with $0.67 < k_{\text{local}}/k_{\text{av}} < 2.1$, for the field waves shown in Fig. 5.

The local nondimensional maximum fluid velocity in 10 crest positions of the wave field shows that $u'_{\max}/c_{\text{local}}$ (with $u' = |(u_1 + U_1, u_2)|$) is a nonlinear function of the local slope $\varepsilon_{\text{local}}$. The function exceeds the local wave slope by 30–40% when it is in the range $\varepsilon_{\text{local}} \sim 0.26 - 0.31$. Figure 5 plots the values of $u'_{\max}/c_{\text{local}}$ obtained in the directional sea together with longcrested irregular wave measurements in the laboratory. The functional relationship between $u'_{\max}/c_{\text{local}}$ and the local wave slope ε is the same in the two different wave fields. The data points fit well with the scaling resulting from the analysis in [5] giving $u_{\max}/c = f(\varepsilon) = \varepsilon \exp(k\eta_{\max})/\sqrt{1+\varepsilon^2} = \varepsilon + \varepsilon^2 + \frac{1}{2}\varepsilon^3 + \ldots$.

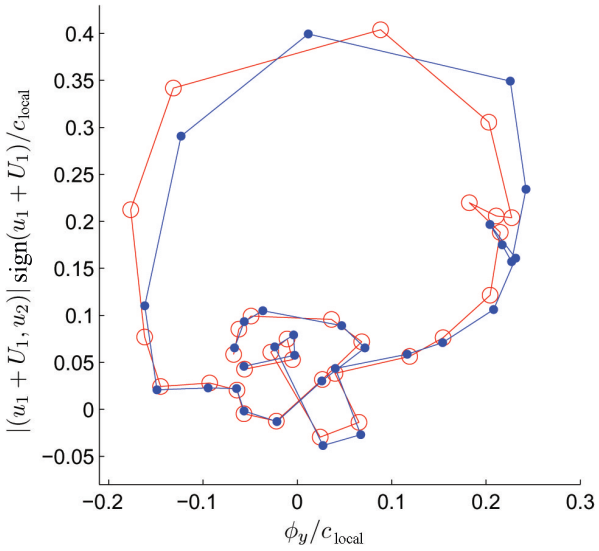

Fig. 4. Hodograph plot with $|(u_1+U_1,u_2)|\text{sign}(u_1+U_1)/c_{\text{local}}$ vs ϕ_y/c_{local}. Calculations with field recording at the aft (line with open circles) and forward (line with dots) positions of the recording plane, for the large event at $x_1 = 4730$ m, $x_2 = 120$ m. Wave propagation from left to right.

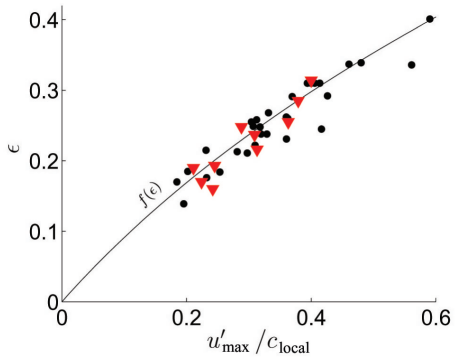

Fig. 5. Maximum horizontal particle velocity scaled by local wave celerity $u'_{\max}/c_{\text{local}}$ with $u' = |(u_1+U_1,u_2)|$, $c_{\text{local}} = \sqrt{g/k_{\text{local}}}\sqrt{1+\varepsilon^2} + U_1, U_1$ current speed vs local wave slope $\varepsilon(=\varepsilon_{\text{local}})$. Laboratory waves (no current): irregular events (dots); directional GOTEX field waves (filled ∇); $f(\varepsilon)(-)$.

Regarding wave breaking, we note that, in the laboratory waves, half of the waves with a wave slope of $\varepsilon \simeq 0.3$ exhibit breaking. The maximum nondimensional horizontal velocity ($u_{\max}/c$) has a value that somewhat exceeds 0.4 in the breaking events. This value corresponds relatively well to a threshold that can be obtained theoretically–numerically in two-dimensional simulations of perturbed Stokes waves, where ε is up to 0.32 and $u_{\max}/c$ up to 0.45, in a recurrent wave scenario.

Finally, we note that the GOTEX waves with the strongest kinematics have a local wave gradient of 0.32 and a nondimensional fluid velocity of 0.40, corresponding to the breaking level observed in the laboratory.

4. CONCLUSIONS

In this paper we have

- presented the steps of a nonlinear mathematical procedure for obtaining, from elevation measurements in the field (and in the laboratory), the nonlinear orbital velocity in directional seas, including the effect of a current;
- used as velocity references, either $c_{\rm av} = \sqrt{g/k_{\rm av}} + U_1$, where $k_{\rm av}$ denotes the average wavenumber of the sea, estimated from rms-values of the elevation gradient and the elevation, or $c_{\rm local} = \sqrt{(g/k_{\rm local})(1+\varepsilon_{\rm local}^2)} + U_1$, where $k_{\rm local}$ is obtained from Eq. (17) above and $\varepsilon_{\rm local}$ denotes the maximum of the local elevation gradient, in both cases U_1 denotes the local current;
- numerically evaluated the orbital velocity, particularly its horizontal components, including the effect of nonlinearity and current;
- particularly evaluated $|(u_1+U_1, u_2)|\text{sign}(u_1+U_1)/c_{\rm local}$ vs $\phi_y/c_{\rm local}$;
- plotted the maximum of $(u_1+U_1)/c_{\rm local}$ in several wave events in the field, including the effect of a current, versus the local nonlinearity $\varepsilon = \varepsilon_{\rm local}$, comparing to the maximum of $u_1/c_{\rm local}$ in the laboratory, without current and wind effects, finding about the same functional relationship;
- finally, not discussed if the effect of the current enhances or does not enhance the nonlinearity in the field waves.

ACKNOWLEDGEMENTS

We acknowledge with gratitude Professor W. K. Melville of Scripps Institution of Oceanography, University of California, San Diego, USA, for making available the GOTEX elevation data in the swath RF05153804 used in the analysis presented here. This research was funded by the Research Council of Norway through NFR191204/V30 “Wave-current-body interaction”.

REFERENCES

1. Clamond, D. and Grue, J. A fast method for fully nonlinear water wave computations. *J. Fluid Mech.*, 2001, **447**, 337–355.
2. Fructus, D., Clamond, D., Grue, J., and Kristiansen, Ø. An efficient model for three-dimensional surface wave simulations. Part I. Free space problems. *J. Comput. Phys.*, 2005, **205**, 665–685.
3. Grue, J. On four highly nonlinear phenomena in wave theory and marine hydrodynamics. *Appl. Ocean Res.*, 2002, **24**, 261–274.
4. Grue, J. and Jensen, A. Orbital velocity and breaking in steep random gravity waves. *J. Geophys. Res.*, 2012, **117**, C07013.
5. Grue, J., Clamond, D., Huseby, M., and Jensen, A. Kinematics of extreme waves in deep water. *Appl. Ocean Res.* 2003, **25**, 355–366.
6. Romero, L. and Melville, W. K. Airborne observations of fetch-limited waves in the Gulf of Tehuantepec. *J. Phys. Oceanogr.*, 2010, **40**, 441–645.

Realistliku lainevälja üksiklainete kinemaatiliste parameetrite arvutamine veepinna salvestustest

John Grue

On esitatud mittelineaarne arvutusmeetod, mis võimaldab pinnalainete kinemaatilised parameetrid leida veepinna asendi muutumise salvestustest. Probleem on lahendatud realistlike laineväljade ja olukorra jaoks, mil laineväljaga kaasneb hoovus. Metoodika on verifitseeritud laboritingimustes genereeritud laineväljade jaoks ja rakendatud Tehuantepeci lahes 2004. aasta eksperimendi GOTEX raames salvestatud veepinna asendi andmestike analüüsiks.